Journal of Magnetic Resonance 300 (2019) 142–148

Contents lists available at ScienceDirect

Journal of Magnetic Resonance

journal homepage: www.elsevier.com/locate/jmr

Maximizing nuclear hyperpolarization in pulse cooling under MAS

Snædís Björgvinsdóttir, Brennan J. Walder, Nicolas Matthey, Lyndon Emsley

Institut des Sciences et Ingénierie Chimiques, Ecole Polytechnique Fédérale de Lausanne (EPFL), CH-1015 Lausanne, Switzerland

ARTICLE INFO

Article history:
Received 29 November 2018
Revised 14 January 2019
Accepted 22 January 2019
Available online 25 January 2019

Keywords:
Solid-state NMR
Dynamic nuclear polarization
Cross-polarization
Spin diffusion

ABSTRACT

It has recently been shown how dynamic nuclear polarization can be used to hyperpolarize the bulk of proton-free solids. This is achieved by generating the polarization in a wetting phase, transferring it to nuclei near the surface and relaying it towards the bulk through homonuclear spin diffusion between weakly magnetic nuclei. Pulse cooling is a strategy to achieve this that uses a multiple contact cross-polarization sequence for bulk hyperpolarization. Here, we show how to maximize sensitivity using the pulse cooling method by experimentally optimizing pulse parameters and delays on a sample of powdered SnO_2. To maximize sensitivity we introduce an approach where the magic angle spinning rate is modulated during the experiment: the CP contacts are carried out at a slow spin rate to benefit from faster spin diffusion, and the spin rate is then accelerated before detection to improve line narrowing. This method can improve the sensitivity of pulse cooling for ^{119}Sn spectra of SnO_2 by an additional factor of 3.5.

1. Introduction

We have recently shown how proton-free solids can be hyperpolarized using dynamic nuclear polarization (DNP) to provide significant signal enhancements in magic-angle-spinning (MAS) NMR experiments [1]. As shown in the schemes in Fig. 1, the method relies on (i) hyperpolarization of weakly magnetic nuclei at the surface of the substrate, and (ii) transport of hyperpolarization from the surface of the substrate to the bulk by spin diffusion among those weakly magnetic nuclei. To achieve this, we have previously described two approaches to implementation of the underlying concept. The first is through direct DNP from polarization agents located in a wetting phase near the surface of the materials to nuclei of the substrate located near the surface. The second is a so-called "pulse cooling" strategy which uses a multiple-contact type cross-polarization sequence [2,3] in which each successive CP step reestablishes thermal contact with the hyperpolarized protons in the wetting phase, and thus maintains a low surface spin temperature. In both cases the polarized spins of the substrate at the surface then undergo slow spontaneous spin diffusion to transport polarization into the bulk, hence also lowering the overall spin temperature. This process becomes especially efficient when the nuclear T_1 values in the substrate are comparatively long, and overall signal enhancements of up to a factor 50 were obtained for ^{119}Sn in SnO_2, and factors ranging from 2 to 85 for materials containing ^{31}P, ^{113}Cd, and ^{29}Si with T_1 values ranging from 200 to 10^5 s.

Multiple-contact CP sequences have been used to obtain quantitative ^{13}C MAS spectra [4], to increase polarization transfer in non-spinning samples [5], and to improve polarization transfer and enhance signals of powders [6].

The pulse cooling scheme used to polarize proton free solids is shown in Fig. 1E and includes flip-forward, flip-back [7], spin-locking, and spin diffusion elements. Each of these elements introduces parameters, as well as the number of CP contacts, that must be set properly in order to maximize sensitivity.

Here we experimentally investigate the relative importance of the various parameters in the pulse cooling sequence. We find that, in general, the sequence tolerates relatively large variations of most of the parameters without compromising sensitivity, and we find that the most critical parameters are the radio-frequency field amplitudes during the CP steps. In particular, in line with the expectation that polarization is relayed by spin diffusion between the weakly magnetic species [1], we find that the best way to cool the bulk is to polarize the sample at a low spinning rate, where spin diffusion is relatively efficient, and then to accelerate the rate of sample spinning prior to detection, which improves line narrowing and thus sensitivity during detection. With this modulation of the rotation rate during the experiment, we improve upon the already impressive sensitivity of the pulse cooling experiment by an additional factor of over 3.5 for ^{119}Sn in SnO_2.

2. Experimental

The batch of SnO_2 (abcr GmbH) powder used to prepare DNP samples was described in our previous work [1]. The samples were

https://doi.org/10.1016/j.jmr.2019.01.011
1090-7807/

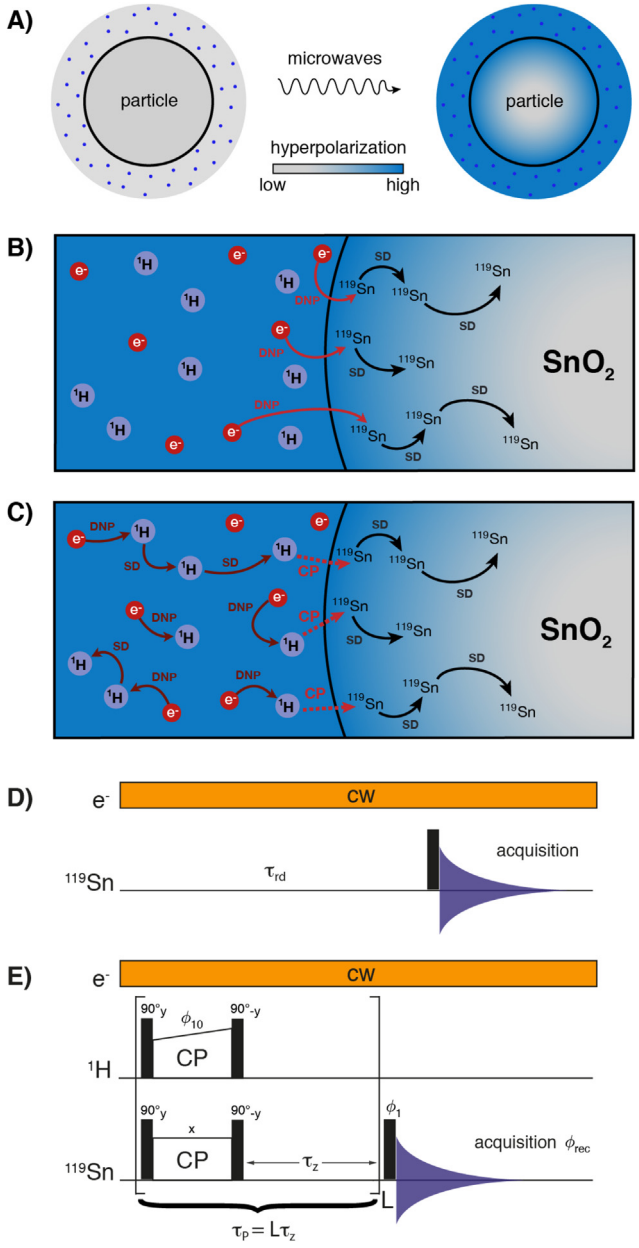

Fig. 1. (A) Schematic representation of hyperpolarization by relay from the surface. (B) Direct polarization of ^{119}Sn near the surface, followed by spin diffusion. (C) Hyperpolarization of surface ^{119}Sn by CP, followed by spin diffusion. (D) Pulse sequence for direct DNP. (E) Pulse cooling sequence using multiple-contact CP. Phase cycle ϕ_{10} = x, ϕ_1 and ϕ_{rec} = [y −y]. Phase cycling can be adjusted to select only ^{1}H sourced magnetization: ϕ_{10} = [x −x], ϕ_{rec} = [y −y] and ϕ_1 = y.

made by impregnating [8,9] the SnO_2 powder (having particle sizes on the order of 1 μm) with a 16 mM solution of TEKPol [10] radical dissolved in 1,1,2,2-tetrachloroethane (TCE). The ratio in the formulations was approximately 10 μL radical solution to 40 mg of powder. The samples were deoxygenated with three thawing cycles to improve DNP enhancements [11,12].

Solid-state NMR experiments were carried out on a 9.4 T Bruker Avance III spectrometer coupled with a 263 GHz microwave source [13]. The samples were spun in a 3.2 mm low-temperature MAS DNP probe, at temperatures around 90 K. The gyrotron collector current was adjusted to optimize the ^{1}H solvent signal enhancement. Radiofrequency field amplitudes of 100 kHz and a 2 ms contact time were used for cross-polarization, unless otherwise specified. The ^{1}H rf field amplitude was ramped from 90% to 100% during CP, to increase polarization transfer efficiency. Presaturation pulses were applied on both the ^{1}H and ^{119}Sn channels prior to the first polarization transfer. For the alternating spin rate version of pulse cooling, the spin rate changes were controlled manually. More details and pulse programs are given in SI.

3. Results and discussion

3.1. Efficiency in pulse cooling

In the pulse sequence of Fig. 1E, multiple cross-polarization contacts repeatedly hyperpolarize the surface of the sample particles by DNP during the polarization period τ_P ($\tau_P = L\tau_z$). The CP blocks consist of a $90°_y$ excitation pulse followed by spin-locks along x on both channels, followed by a $90°_{-y}$ flip-back storage pulse that puts the magnetization back along the direction of the main magnetic field. Each block is then followed by a delay, τ_z, that allows protons in the wetting phase to repolarize under DNP while spin diffusion between the weakly magnetic nuclei transfers hyperpolarization from the surface of the sample particle towards the bulk [1].

The overall efficiency of this method is governed by the DNP enhancements that can be obtained, either for ^{1}H nuclei close to the surface in the wetting medium for pulsed cooling, or for the weakly magnetic nuclei at the surface of the sample particles for the direct DNP approach. These surface enhancements can vary significantly, depending on the substrate and the formulation. These effects are currently the subject of intense study [14–18]. Even here, where a single formulation is used throughout the study, we observed significant variability in DNP enhancements across experimental sessions, with the ^{1}H enhancement of TCE at 8 kHz MAS ranging between 140 and 270. However, the surface DNP enhancement translates directly into the overall enhancement in a manner independent from the pulse sequence parameters, so we do not consider this further here, though it is important to keep in mind when establishing comparisons across different samples.

In a simplified model of the polarization build-up, approximating the most usual situation where the spin diffusion length is smaller than the characteristic length scale of the particles, we assume that each "flipforward-CP-flipback" cooling burst adds one unit of magnetization, with the ensuing interval of longitudinal storage τ_z chosen to be long enough such that this added magnetization is entirely transported into the bulk. During this interval, a fraction of the accumulated magnetization is lost due to relaxation. In the limit $\tau_z \ll T_1$, the amount of bulk magnetization that remains after τ_z is determined by multiplying the preexisting magnetization by the relaxation retention factor f_{relax}. In a similar fashion, we can assign a retention factor f_{burst} to each cooling burst to represent the amount of bulk magnetization that is retained across the burst of pulses, which is less than unity due to imperfections in the short pulse elements and $T_{1\rho}$ processes. Then the amplification of bulk polarization after L cycles during acquisition is given by

$$F_{bulk} = f_{relax}\frac{1-(f_{relax}f_{burst})^L}{1-f_{relax}f_{burst}}, \quad (1)$$

which becomes

$$F_{bulk} = \frac{f_{relax}}{1-f_{relax}f_{burst}} \quad (2)$$

at steady-state. Generally, between ten and twenty cooling bursts are used for pulse cooling and steady-state is approached. Using estimated values for the experimental parameters in Eq. (2), we therefore see that small changes in the retention factors will lead to significant overall losses in the final signal intensity. For example,

if we take f_{relax} = 0.98 (such that τ_z/T_1 is about 2%), and assume that each cooling burst is 98% efficient (f_{burst} = 0.98), we find that F_{bulk} = 24.7. On the other hand, if each cooling burst is 2% less efficient in this scenario, (f_{burst} = 0.96), then F_{bulk} = 16.6, and another factor one-third of the potential magnetization build-up is lost.

In this light, it is imperative to understand the relative importance of the pulse cooling sequence parameters which influence retention of magnetization, in addition to those parameters which modulate spin diffusion. In the following sections we look into the optimization of pulse parameters and delays in pulse cooling.

3.2. Effects of CP efficiency on pulse cooling

Fig. 2A and B show the effect of different ^{119}Sn spin-locking rf field amplitudes and contact times on the signal-to-noise ratio of ^{119}Sn spectra in SnO_2. The normalized sensitivity, defined as the signal-to-noise ratio of the spectrum divided by the mass of the bulk material in the rotor and the square root of the experiment time, is increased by around 30% when going from amplitudes of 50–125 kHz with a spin lock duration of τ_{CP} = 400 μs, with an even larger change observed when the contact time is longer. This is a striking improvement which can be rationalized by looking at the simplified model of polarization of the preceding section in greater physical detail. Changing the rf amplitude can affect the extent of polarization transfer to surface ^{119}Sn species by CP or the burst retention factor f_{burst}. A change in CP transfer efficiency is not sufficient to explain the factor of roughly one-third sensitivity gain with higher spin-locking fields, since the effect is maintained for contact times which deviate greatly from the optimum value of τ_{CP} = 2 ms, as shown in Fig. 2A.

As is well-known, the rf amplitude has a strong influence on $T_{1\rho}$. A ν_1^2 dependence might be expected for a network of like spin-1/2 nuclei in a rigid solid [19,20], like ^{119}Sn in SnO_2. This leads us to expect that $T_{1\rho}$ (^{119}Sn) at ν_1(^{119}Sn) = 125 kHz is over six times larger than it is for ν_1(^{119}Sn) = 50 kHz. If contributions to f_{burst} other

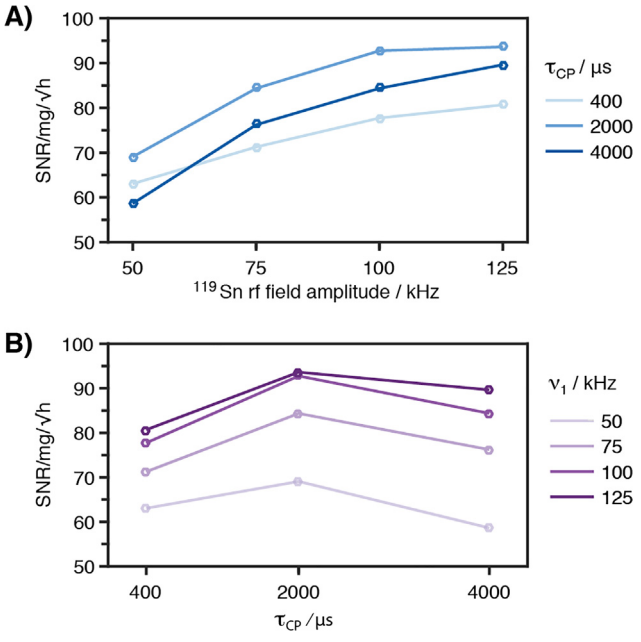

Fig. 2. Sensitivity (including intrinsic build-up of ^{119}Sn) as a function of (A) spin-locking amplitude, ν_1, and (B) as a function of spin lock duration, τ_{CP}. Pulse cooling parameters: τ_z = 10 s and τ_P = 120 s. The lines connecting the data points are a guide for the eye. For each of the different ^{119}Sn spin-locking fields, the amplitude of the ^{1}H spin-locking field was recalibrated using conventional (DNP enhanced) CP spectra to ensure the optimum matching conditions are fulfilled.

than rotating frame relaxation are ignored, then $f_{burst} \approx 1 - \tau_{CP}/T_{1\rho}$, (assuming $\tau_{CP} \ll T_{1\rho}$), in which case f_{burst} draws substantially closer to unity when going from 50 kHz to 125 kHz (from 0.94 to 0.99). Considering that there are other sources that may contribute to loss of retention (for example fluctuating effective fields (such as those due to shielding anisotropy) leading to a less than expected gain in $T_{1\rho}$ (^{119}Sn), phase and amplitude transients, flanking pulse imperfections, etc.), any actual gain in the retention factor f_{burst} is likely to be much smaller. Nevertheless, as discussed in the previous section, small changes in $f_{burst.}$ are still capable of producing large changes in the overall sensitivity, and we identify the $T_{1\rho}$ contribution to f_{burst} as the most likely explanation of the large overall sensitivity gains when strong spin-locking fields are used in pulse cooling.

We also note that, in addition to the trend towards better pulse cooling sensitivity with increasing rf amplitude shown in Fig. 2A, stronger spin-locking fields also attenuate the performance drop-off at contact times which are longer than optimal, as shown in Fig. 2B. This is consistent with the idea of a significant $T_{1\rho}$ (^{119}Sn) contribution to f_{burst}.

Regardless of details, higher spin locking fields should not, in general, inhibit efficient CP transfer, but they should allow for greater retention of magnetization (higher f_{burst} values) due to less efficient $T_{1\rho}$ relaxation. Thus, as a general rule, we conclude that one should use the highest spin-locking amplitudes that can be safely handled by the equipment.

3.3. Tolerance to misset and offset effects

The ^{119}Sn spectrum of SnO_2 only has one chemical shift, but its offset from the transmitter frequency can be used to simulate the effect on a system with more than one distinct chemical shift, where off-resonance irradiation is inevitable. Fig. 3 shows how the signal intensity in the ^{119}Sn spectra of SnO_2 changes when the ^{119}Sn pulses are applied up to ±100 kHz off resonance and when the pulse and spin lock amplitudes are misset (by ±20 kHz from an ideal value of 100 kHz). As expected, we see a gradual decline in intensity as a function of both offset and misset. For offset we note that >80% of the on-resonance intensity for a well calibrated 100 kHz 90° pulse is retained over a region of about 30 kHz. For misset of the pulse flip angle and the spin lock amplitude, at least 60% of the on-resonance intensity is retained for ±10% change in ^{119}Sn channel rf amplitude.

An asymmetric appearance of the offset profiles about zero is notable, and particularly prominent for negative rf amplitude missets. In a conventional CP experiment, where the only pulse on the observe channel is the contact pulse, offset profiles are expected to be symmetric about zero. This is because the transverse component of magnetization is proportional to $\cos(\nu_{off}/\nu_{eff})$, which is an even function of the sign of the offset frequency ν_{off} (ν_{eff} refers to the effective field amplitude), and misset only affects the magnitude of the transfer. Multiple contact CP sequences such as pulse cooling, however, introduce the need to control the trajectory of magetization across each CP burst. After each storage delay, the magnetization must be placed along the effective field axis, *and* returned to longitudinal storage after the transfer step is complete. Since the effective field direction depends on the sign of the offset, the performance of flip-forward and flip-back pulse elements, and the burst as a whole, also depends on the sign of the offset. For example, at severe negative rf amplitude missets, the single pulse elements have a flip-angle that is less than 90°, such that after excitation the magnetization is best aligned with a spin-locking field that possesses a positive offset. This leads to the "right-weighted" offset profile at 80 kHz rf amplitude shown in Fig. 3.

Composite pulses can make pulse sequences more tolerant to resonance offset and misset pulse flip-angles [21]. Recently, Duan

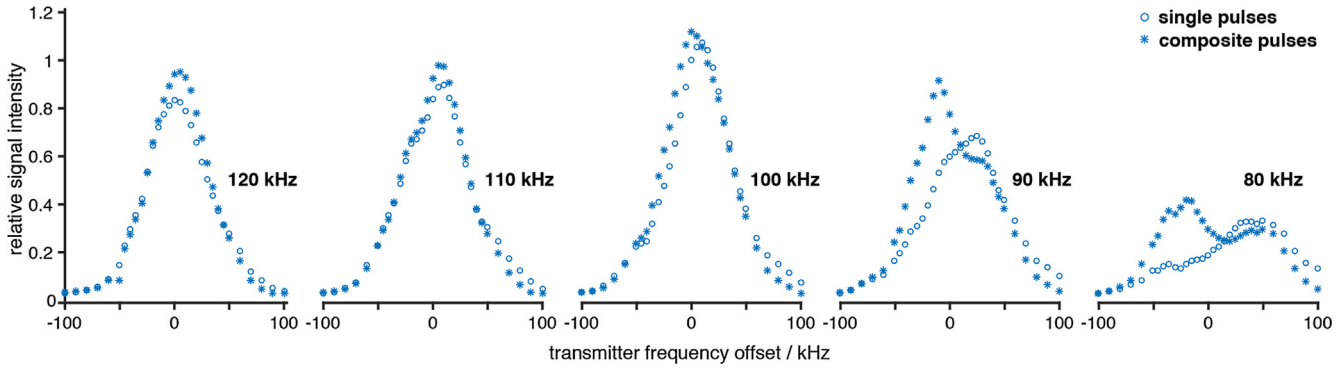

Fig. 3. Effect of carrier frequency offset on the intensity of the ^{119}Sn signal in a pulsed cooling spectrum of impregnated SnO_2 spinning at 8 kHz, for ^{119}Sn rf frequency amplitudes ranging from 80 to 120 kHz, obtained with either single or composite pulses. The signal intensity is relative to that of a 100 kHz 90° pulse at 0 offset. Pulse cooling parameters: τ_z = 10 s and τ_P = 120 s.

and Schmidt-Rohr developed a pair of composite pulses for excitation and storage in multiple contact CP with composite pulses on the observe channel [22]. The excitation pulse becomes $90°_{270}180°_{45}$. Similarly, the storage pulse becomes $180°_{135}90°_{270}$. This pair of pulses is respectively designed to place the magnetization along, and restore magnetization from, the effective spin-locking field direction under conditions of offset and misset. In our experiments for pulse cooling, we find that these composite pulses (on the ^{119}Sn channel; composite pulses have not been tested on the ^{1}H channel) usually provide higher overall intensity. As might be expected, the improvement is most noticeable in cases where the rf field amplitude on the ^{119}Sn channel is lower than 100 kHz, where the spin-locking field is both less efficient and the nominal 90° pulse has a flip-angle that is too small. As an example, for 90 kHz ^{119}Sn amplitude and roughly −20 kHz transmitter offsets, the composite pulses can provide improvements up to a factor of 1.9 relative to the version implementing single pulses. We also note that these composite pulses tend to improve the symmetry of the offset profiles, particularly for the offset profile at 80 kHz rf amplitude. This is to be expected on the basis of their design principles.

Applying an amplitude ramp on one of the two B_1 fields during CP is known to increase the efficiency of polarization transfer [23–26]. The results presented here all have the ^{1}H rf field amplitude ramped from 90 to 100% during each spin-locking period. Adiabatic ^{1}H frequency sweeps [27] broaden the HH matching condition and might make the pulse cooling experiment even more tolerant to misset of the spin-locking fields. However, we have not found any significant improvement using frequency sweeps (see Fig. S1).

3.4. Choice of polarization and repetition times

In addition to pulse elements, the pulse cooling sequence also contains spin diffusion elements that need to be set properly in order to maximize polarization relay into the bulk of the material. The polarization gain is sensitive to the balance between the build-up rate of the compound, the rate of homonuclear spin diffusion, and the rate of T_1 relaxation. Therefore, selection of the polarization period, τ_P, and the storage interval, τ_z, is important for efficient pulse cooling.

These parameters can be optimized experimentally for each spin rate as shown in Fig. 4. The delay after each CP contact, τ_z, should in general be longer than the ^{1}H build-up time in the wetting phase, $T_{B,H}$. The polarization period τ_P ($\tau_P = L\tau_z$) should be long enough so that hyperpolarization transferred from the surface by spin diffusion can accumulate in the bulk, but shorter than the intrinsic T_1 of ^{119}Sn in SnO_2. We find that there is a correlation between parameters, the value of τ_z which leads to optimal sensitivity increases as τ_P increases. Nonetheless, taking 8 kHz MAS as an example, over 70% of the maximum sensitivity is retained over a range of τ_z = 5–50 s and τ_P = 100–500 s. The changes in sensitivity are observable, but not significant over a range of values of τ_P, τ_z and L, which shows that the method is fairly tolerant to imprecise setting of these values, at least when sensitivity enhancements are high. In general, setting the number of CP steps, L, to be 10–20 is a good rule of thumb. Exceptions might be when T_1 is comparable to the build-up time, in which case a smaller number of cycles will be preferred, or when the diffusion constant is very large, in which case shorter τ_z might be required with a larger number of repetitions.

The difference in the optimum τ_P and τ_z values for different spin rates can be explained by spinning induced changes in the intrinsic build-up of bulk ^{119}Sn polarization relative to the build-up rates of the surface protons. The intrinsic build-up of bulk ^{119}Sn is defined as the contribution from ^{119}Sn that does not arise by CP from hyperpolarized protons, i.e., it includes signal from hyperpolarized ^{119}Sn originating from direct DNP (with or without relay), or thermally polarized ^{119}Sn.

Fig. 5 plots the normalized sensitivity values of the bulk ^{119}Sn signal in SnO_2 spinning at 8 kHz, obtained with different phase cycles that selectively include or exclude the intrinsic contribution to the bulk signal. The sensitivities are plotted as a function of τ_z for four different polarization delays, τ_P = 120 s, 240 s, 360 s, and 480 s. The build-up of proton polarization in the wetting phase by DNP is orders of magnitude faster than that of the build-up of thermal ^{119}Sn polarization, which is why the sensitivities are similar for values of τ_z up to the build-up rate of proton magnetization (here up to about 10 s). For longer τ_z the additional signal from polarization pathways including direct ^{119}Sn DNP becomes significant, and leads to significantly higher sensitivity than the ^{1}H sourced experiment.

3.5. Spin-up pulse cooling

The rate of spin diffusion slows down as the MAS rate is increased, when homonuclear dipolar interactions are averaged more efficiently [28–31]. However, sensitivity is lower at slow spin rates due to an increase in the number of spinning side bands in the presence of significant chemical shift anisotropy. In light of this, we present a version of pulse cooling (Fig. 6A) where the multiple CP contacts are performed at a low MAS rate, to benefit from more efficient spin diffusion, while the FID is detected at a higher spin rate, to maximize sensitivity where the spinning side bands are reduced. The modified pulse sequence has two additional

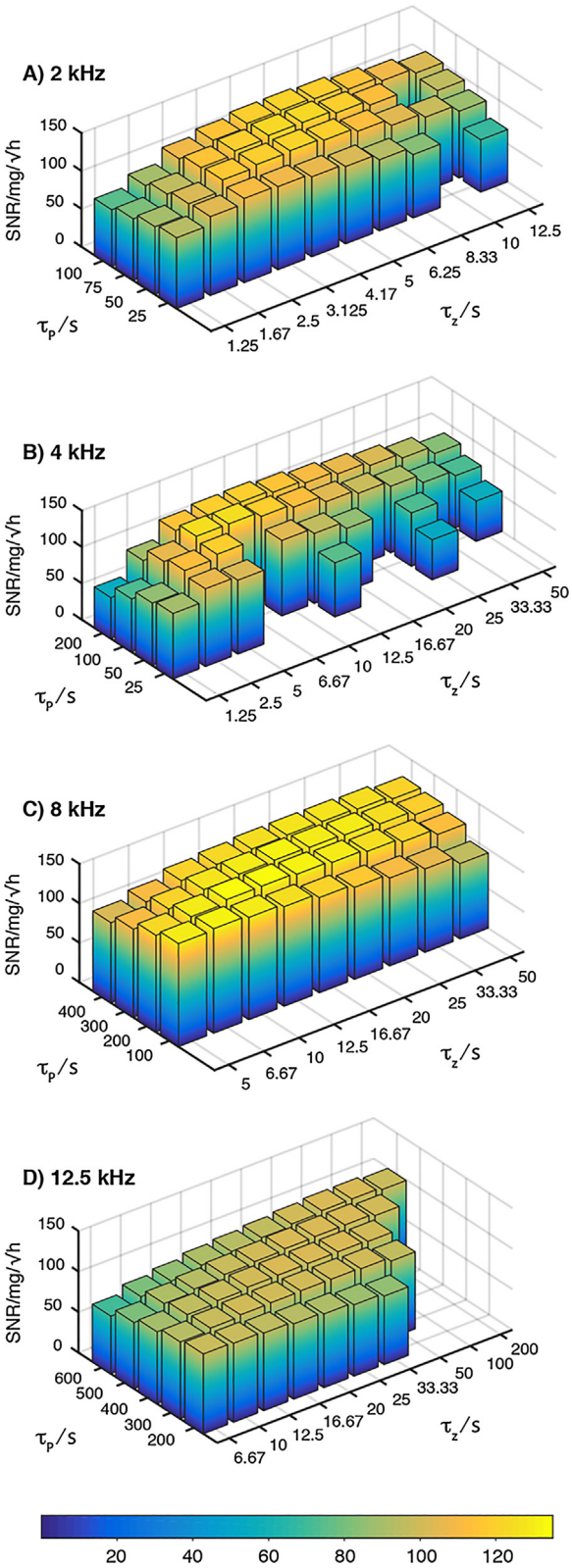

Fig. 4. Optimization of the fully normalized sensitivity of the ^{1}H-^{119}Sn DNP enhanced spectra of SnO_2 impregnated with 16 mM TEKPol in TCE using the pulse cooling experiment for NMR signal acquisition. The fully normalized sensitivity is defined as signal-to-noise ratio divided by the mass of the bulk material in the rotor and the square root of the experiment time. The spectra were recorded at a MAS rate of (A) 2 kHz, (B) 4 kHz, (C) 8 kHz and (D) 12.5 kHz. The radio-frequency field amplitude during CP was adjusted to compensate for changes in transfer efficiency at each different spin rate.

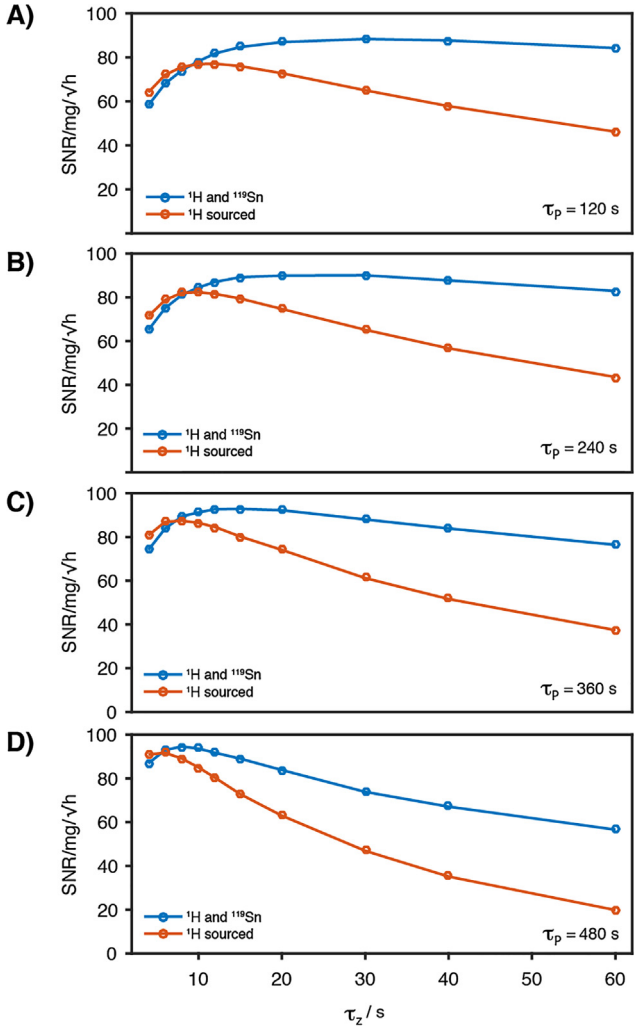

Fig. 5. Comparison of the normalized sensitivity between pulse cooling experiments including intrinsic build-up of ^{119}Sn (^{1}H and ^{119}Sn, blue) and pulse cooling excluding intrinsic ^{119}Sn build-up (^{1}H sourced, red), at four different polarization delays, τ_p. The sample is SnO_2 impregnated with 16 mM TEKPol in TCE, spinning at 8 kHz MAS. The CP spin lock amplitude was ν_1 = 125 kHz and the contact time 2 ms. Solid lines are a guide for the eye. See Fig. S2 for different spin lock parameters.

delays, τ_{up} and τ_{down}, which are used to change the MAS rate. We note that spin rate acceleration and deceleration during an experiment has been proposed previously for correlating static patterns to isotropic chemical shifts [32], and for broadening CP matching conditions [33]. It has also been used in the context of DNP before (but in the opposite sense, polarizing with a spinning sample and detecting on a static sample for quadrupolar nuclei) [34].

Fig. 6C shows the results obtained for a series of combinations of spinning rates. We see that a polarization spin rate, ν_{pol}, of 500 Hz results in the highest sensitivity for all acquisition spin rates, ν_{aq}. Polarizing at higher spin rates provides less of a gain, as the dipolar couplings are averaged out more efficiently, slowing down spin diffusion. When the MAS rate is higher than the strength of the dipolar couplings the rate of spin diffusion is usually inversely proportional to ν_r [29–31,35]. In this regime we find, for example, that if the spin rate is decreased from 8 kHz to 4 kHz during the polarization period, the sensitivity goes from 62 to 101 (ν_{aq} = 8 kHz), which is not far from the expected factor of 2, especially when the additional spinning sidebands at 4 kHz are

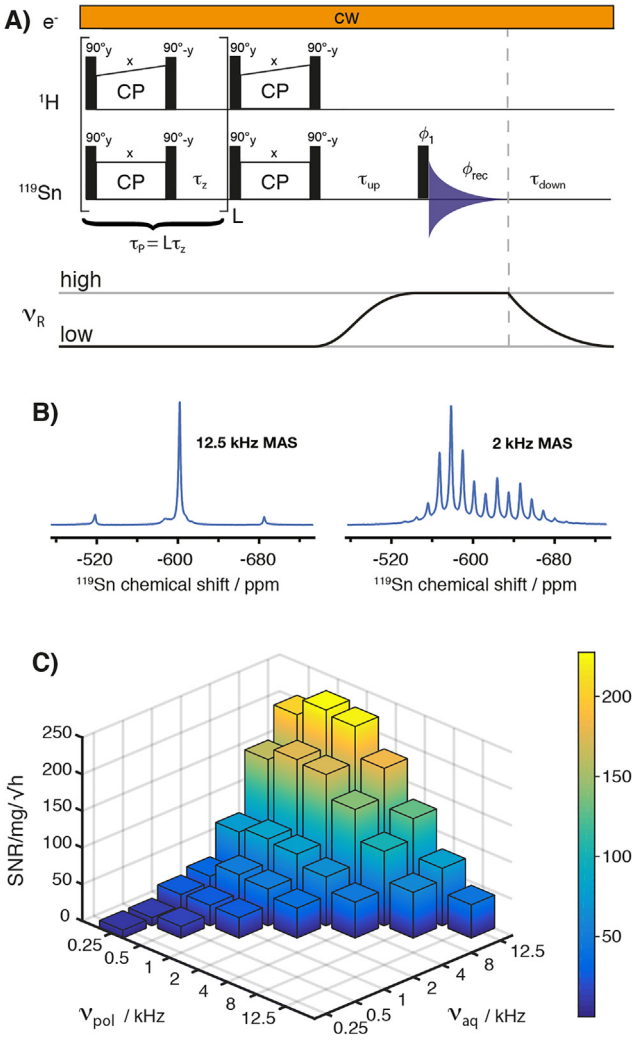

Fig. 6. (A) The pulse cooling sequence with MAS rate changes before and after acquisition. (B) ^{1}H-^{119}Sn CP spectra of SnO_2 at two different spin rates. (C) Sensitivity enhancements observed by using the pulse sequence in panel A. The numerical values which have been plotted are given in Table S2. The pulse cooling parameters for each experiment are optimal for ν_{pol} and are given in Table S3.

considered. The pulse cooling parameters, τ_P and τ_z, used in each experiment are optimal for the spin rate used during the polarization period, ν_{pol}.

We also note that polarizing at 250 Hz also results in lower sensitivity than at 500 Hz. This is possibly because 250 Hz is less than the strength of the estimated dipolar couplings in SnO_2, and hence spin diffusion is entering the quasi-static regime. It is known that slow spinning rates usually enhance spin diffusion rates as compared to the spin diffusion rate in a static sample [36,37].

For a single spin rate, the balance between the rate of diffusion and the efficiency of CSA averaging is most favorable for SnO_2 at 8 kHz (it is the highest peak on the diagonal of Fig. 6C).

The maximum length of the acceleration delay, τ_{up}, imposes a practical limitation on the difference between the high and low spin rate. If the delay is too long, part of the signal will be lost to relaxation effects. Here, all the acceleration and deceleration delays were 30 s which allows sufficient time to go from 250 Hz to 12500 Hz.

We note that the spin rate modulation proposed here can in principle also be used in the direct DNP approach, by spinning up at the end of the relatively long recycle delay.

4. Conclusions

We have shown how parameters relating to specific elements in the pulse cooling method can be optimized experimentally. This is demonstrated on SnO_2, and we find that, in general, well calibrated pulses and high spin lock powers are beneficial for obtaining the best sensitivity. We also show how to select the delays and number of contacts in the pulse sequence in order to maximize polarization relay to the bulk.

A variation of pulse cooling is presented where the rotation rate of the sample is modulated during the experiment, providing an additional gain in sensitivity of a factor of 3.5 for ^{119}Sn in SnO_2.

In summary, as a general guide for navigating the multidimensional parameter space presented in this work, we issue the following recommendations for setting up pulse cooling on an unknown sample:

(i) use the highest spin locking power that can be safely tolerated by the instrument;
(ii) ensure that the pulses which flank the CP bursts are calibrated well, using the composite pulses of Duan and Schmidt-Rohr [22] to further improve robustness toward misset and offset if needed;
(iii) set the polarization delay τ_P to be on the order of the intrinsic nuclear T_1 of the species that is to be detected;
(iv) set the number of CP contacts to between 10 and 20; and
(v) spin the sample slowly, using the spin-up version of the experiment to improve resolution and sensitivity if necessary.

Acknowledgements

This work was supported by Swiss National Science Foundation Grants No. 200021_160112 & 200020_178860.

Appendix A. Supplementary material

Supplementary data to this article can be found online at https://doi.org/10.1016/j.jmr.2019.01.011.

References

[1] S. Bjorgvinsdottir, B.J. Walder, A.C. Pinon, L. Emsley, Bulk nuclear hyperpolarization of inorganic solids by relay from the surface, J. Am. Chem. Soc. 140 (25) (2018) 7946–7951.
[2] A. Pines, M.G. Gibby, J.S. Waugh, Proton-enhanced NMR of dilute spins in solids, J. Chem. Phys. 59 (2) (1973) 569–590.
[3] S.M. Zhang, X.L. Wu, M. Mehring, Successive polarization under mismatched Hartmann-Hahn condition, Chem. Phys. Lett. 166 (1) (1990) 92–94.
[4] R.L. Johnson, K. Schmidt-Rohr, Quantitative solid-state 13C NMR with signal enhancement by multiple cross polarization, J. Magn. Reson. 239 (2014) 44–49.
[5] A.A. Nevzorov, Ergodicity and efficiency of cross-polarization in NMR of static solids, J. Magn. Reson. 209 (2) (2011) 161–166.
[6] J. Raya, B. Perrone, J. Hirschinger, Chemical shift powder spectra enhanced by multiple-contact cross-polarization under slow magic-angle spinning, J. Magn. Reson. 227 (2013) 93–102.
[7] J. Tegenfeldt, U. Haeberlen, Cross polarization in solids with flip-back of I-spin magnetization, J. Magn. Reson. (1969) 36 (3) (1979) 453–457.
[8] A. Lesage, M. Lelli, D. Gajan, M.A. Caporini, V. Vitzthum, P. Miéville, J. Alauzun, A. Roussey, C. Thieuleux, A. Mehdi, G. Bodenhausen, C. Coperet, L. Emsley, Surface enhanced NMR spectroscopy by dynamic nuclear polarization, J. Am. Chem. Soc. 132 (44) (2010) 15459–15461.
[9] A.J. Rossini, A. Zagdoun, M. Lelli, A. Lesage, C. Coperet, L. Emsley, Dynamic nuclear polarization surface enhanced NMR spectroscopy, Acc. Chem. Res. 46 (9) (2013) 1942–1951.
[10] A. Zagdoun, A.J. Rossini, M.P. Conley, W.R. Gruning, M. Schwarzwalder, M. Lelli, W.T. Franks, H. Oschkinat, C. Coperet, L. Emsley, A. Lesage, Improved dynamic nuclear polarization surface-enhanced NMR spectroscopy through controlled incorporation of deuterated functional groups, Angew. Chem. Int. Ed. Engl. 52 (4) (2013) 1222–1225.

[11] D.J. Kubicki, A.J. Rossini, A. Purea, A. Zagdoun, O. Ouari, P. Tordo, F. Engelke, A. Lesage, L. Emsley, Amplifying dynamic nuclear polarization of frozen solutions by incorporating dielectric particles, J. Am. Chem. Soc. 136 (44) (2014) 15711–15718.
[12] M. Rosay, Ph.D. Thesis. Massachusetts Institute of Technology, Cambridge, MA, 2001.
[13] M. Rosay, L. Tometich, S. Pawsey, R. Bader, R. Schauwecker, M. Blank, P.M. Borchard, S.R. Cauffman, K.L. Felch, R.T. Weber, R.J. Temkin, R.G. Griffin, W.E. Maas, Solid-state dynamic nuclear polarization at 263 GHz: spectrometer design and experimental results, Phys. Chem. Chem. Phys. 12 (22) (2010) 5850–5860.
[14] F.A. Perras, L.L. Wang, J.S. Manzano, U. Chaudhary, N.N. Opembe, D.D. Johnson, I.I. Slowing, M. Pruski, Optimal sample formulations for DNP SENS: the importance of radical-surface interactions, Curr. Opin. Colloid Interface Sci. 33 (2018) 9–18.
[15] A.J. Rossini, A. Zagdoun, M. Lelli, D. Gajan, F. Rascon, M. Rosay, W.E. Maas, C. Coperet, A. Lesage, L. Emsley, One hundred fold overall sensitivity enhancements for Silicon-29 NMR spectroscopy of surfaces by dynamic nuclear polarization with CPMG acquisition, Chem. Sci. 3 (1) (2012) 108–115.
[16] U. Akbey, B. Altin, A. Linden, S. Ozcelik, M. Gradzielski, H. Oschkinat, Dynamic nuclear polarization of spherical nanoparticles, Phys. Chem. Chem. Phys. 15 (47) (2013) 20706–20716.
[17] R.P. Sangodkar, B.J. Smith, D. Gajan, A.J. Rossini, L.R. Roberts, G.P. Funkhouser, A. Lesage, L. Emsley, B.F. Chmelka, Influences of dilute organic adsorbates on the hydration of low-surface-area silicates, J. Am. Chem. Soc. 137 (25) (2015) 8096–8112.
[18] T. Kobayashi, F.A. Perras, U. Chaudhary, I.I. Slowing, W.Y. Huang, A.D. Sadow, M. Pruski, Improved strategies for DNP-enhanced 2D H-1-X heteronuclear correlation spectroscopy of surfaces, Solid State Nucl. Magn. Reson. 87 (2017) 38–44.
[19] A.G. Redfield, Nuclear magnetic resonance saturation and rotary saturation in solids, Phys. Rev. 98 (6) (1955) 1787–1809.
[20] D.C. Look, I.J. Lowe, Nuclear magnetic dipole-dipole relaxation along static and rotating magnetic fields - application to gypsum, J. Chem. Phys. 44 (8) (1966) 2995–3000.
[21] M.H. Levitt, R. Freeman, NMR population-inversion using a composite pulse, J. Magn. Reson. 33 (2) (1979) 473–476.
[22] P. Duan, K. Schmidt-Rohr, Composite-pulse and partially dipolar dephased multiCP for improved quantitative solid-state 13C NMR, J. Magn. Reson. 285 (2017) 68–78.
[23] M.H. Levitt, D. Suter, R.R. Ernst, Spin dynamics and thermodynamics in solid-state NMR cross polarization, J. Chem. Phys. 84 (8) (1986) 4243–4255.
[24] O.B. Peersen, X.L. Wu, I. Kustanovich, S.O. Smith, Variable-amplitude cross-polarization Mas NMR, J. Magn. Reson. Ser. A 104 (3) (1993) 334–339.
[25] G. Metz, M. Ziliox, S.O. Smith, Towards quantitative CP-MAS NMR, Solid State Nucl. Magn. Reson. 7 (3) (1996) 155–160.
[26] S.R. Hartmann, E.L. Hahn, Nuclear double resonance in rotating frame, Phys. Rev. 128 (5) (1962) 2042–3000.
[27] A.C. Kolbert, A. Bielecki, Broad-band Hartmann-Hahn matching in magic-angle-spinning NMR via an adiabatic frequency sweep, J. Magn. Reson. Ser. A 116 (1) (1995) 29–35.
[28] M.M. Maricq, J.S. Waugh, NMR in rotating solids, J. Chem. Phys. 70 (7) (1979) 3300–3316.
[29] S. Clough, K.W. Gray, Spin diffusion and nuclear magnetic resonance in rotating solids, Proc. Phys. Soc. 80 (6) (1962) 1382.
[30] S. Clough, K.W. Gray, The stochastic theory of the nuclear magnetic resonance line in rotating solids, Proc. Phys. Soc. 79 (3) (1962) 457.
[31] H. Kessemeier, R.E. Norberg, Pulsed nuclear magnetic resonance in rotating solids, Phys. Rev. 155 (2) (1967) 321–337.
[32] R.C. Zeigler, R.A. Wind, G.E. Maciel, The stop-and-go spinning technique in MAS experiments, J. Magn. Reson. 79 (2) (1988) 299–306.
[33] A. Samoson, T. Tuherm, J. Past, Ramped-speed cross polarization MAS NMR, J. Magn. Reson. 149 (2) (2001) 264–267.
[34] D.A. Hirsh, A.J. Rossini, L. Emsley, R.W. Schurko, 35Cl dynamic nuclear polarization solid-state NMR of active pharmaceutical ingredients, Phys. Chem. Chem. Phys. 18 (37) (2016) 25893–25904.
[35] M.E. Halse, A. Zagdoun, J.N. Dumez, L. Emsley, Macroscopic nuclear spin diffusion constants of rotating polycrystalline solids from first-principles simulation, J. Magn. Reson. 254 (2015) 48–55.
[36] R. Challoner, J. Kummerlen, C. McDowell, Spectral spin-diffusion under $n = 0$ rotational resonance, Mol. Phys. 83 (4) (1994) 687–700.
[37] M. Roos, P. Micke, K. Saalwachter, G. Hempel, Moderate MAS enhances local 1H spin exchange and spin diffusion, J. Magn. Reson. 260 (2015) 28–37.